Journal Pre-proof

Revealing extensive inbreeding and less-efficient purging of deleterious mutations in wild Amur tigers in China

Tianming Lan, Haimeng Li, Boyang Liu, Minhui Shi, Yinping Tian, Sunil Kumar Sahu, Liangyu Cui, Nicolas Dussex, Dan Liu, Yue Ma, Weiyao Kong, Shanlin Liu, Jiale Fan, Yue Zhao, Yuan Fu, Qiye Li, Chen Lin, Love Dalén, Huan Liu, Le Zhang, Guangshun Jiang, Yanchun Xu

PII: S1673-8527(24)00336-9

DOI: https://doi.org/10.1016/j.jgg.2024.12.004

Reference: JGG 1435

To appear in: *Journal of Genetics and Genomics*

Received Date: 1 December 2024

Accepted Date: 3 December 2024

Please cite this article as: Lan, T., Li, H., Liu, B., Shi, M., Tian, Y., Sahu, S.K., Cui, L., Dussex, N., Liu, D., Ma, Y., Kong, W., Liu, S., Fan, J., Zhao, Y., Fu, Y., Li, Q., Lin, C., Dalén, L., Liu, H., Zhang, L., Jiang, G., Xu, Y., Revealing extensive inbreeding and less-efficient purging of deleterious mutations in wild Amur tigers in China, *Journal of Genetics and Genomics*, https://doi.org/10.1016/j.jgg.2024.12.004.

Revealing extensive inbreeding and less-efficient purging of deleterious mutations in wild Amur tigers in China

Tianming Lan[a,b,l], Haimeng Li[a,c,d,l], Boyang Liu[a,l], Minhui Shi[c], Yinping Tian[a], Sunil Kumar Sahu[e], Liangyu Cui[a], Nicolas Dussex[f,g,h], Dan Liu[i], Yue Ma[a], Weiyao Kong[j], Shanlin Liu[k], Jiale Fan[a], Yue Zhao[a], Yuan Fu[a], Qiye Li[c], Chen Lin[a], Love Dalén[f,g,h], Huan Liu[b,c,l], Le Zhang[a, *], Guangshun Jiang[a, *], Yanchun Xu[a,b,m, *]

[a] College of Wildlife and Protected Area, Northeast Forestry University, Harbin, Heilongjiang 150040, China

[b] BGI Life Science Joint Research Center, Northeast Forestry University, Harbin, Heilongjiang 150040, China

[c] State Key Laboratory of Agricultural Genomics, BGI-Shenzhen, Shenzhen, Guangdong 518083, China

[d] Heilongjiang Key Laboratory of Complex Traits and Protein Machines in Organisms, Harbin, Heilongjiang 150040, China

[e] BGI Research, Wuhan, Hubei 430074, China

[f] Centre for Palaeogenetics, Svante Arrhenius väg 20C, 10691 Stockholm, Sweden

[g] Department of Zoology, Stockholm University, Stockholm, Sweden

[h] Department of Bioinformatics and Genetics, Swedish Museum of Natural History, Stockholm, Sweden

[i] Heilongjiang Siberian Tiger Park, Harbin, Heilongjiang 150000, China

[j] Jinlin Provincial Academy of Forestry Science, Changchun, Jilin 130033, China

[k] Key Laboratory of Zoological Systematics and Evolution, Institute of Zoology, Chinese Academy of Sciences, Beijing 100101, China

[l] Guangdong Provincial Key Laboratory of Genome Read and Write, BGI-Shenzhen, Shenzhen, Guangdong 518120, China

[m] National Forestry and Grassland Administration Research Center of Engineering Technology for Wildlife Conservation and Utilization, Harbin, Heilongjiang,150040 China

* Corresponding authors.

Email addresses: zhangl_0811@163.com (L. Zhang); jgshun@126.com (G. Jiang); xu_daniel@163.com (Y. Xu).

[1]These authors contributed equally to this work.

ABSTRACT

Inbreeding increases genome homozygosity within populations, which can exacerbate inbreeding depression by exposing homozygous deleterious alleles that are responsible for declines in fitness traits. In small populations, genetic purging that occurs under pressure of natural selection acts as an opposing force, contributing to a reduction of deleterious alleles. Both inbreeding and genetic purging are paramount in the field of conservation genomics. The Amur tiger (*Panthera tigris altaica*) lives in small populations in the forests of Northeast Asia and is among the most endangered animals on the planet. Using genome-wide assessment and comparison, we reveal substantially higher and more extensive inbreeding in wild Amur tigers (F_{ROH} = 0.50) than in captive individuals (F_{ROH} = 0.24). However, a relatively reduced number of loss-of-function mutations in wild Amur tigers was observed when compared with captive individuals, indicating a genetic purging of relatively large-effect inbreeding load. The higher ratio of homozygous mutation load and number of fixed damaging alleles in the wild population indicate a less-efficient genetic purging, with purifying selection also contributing to this process. These findings provide valuable insights for future conservation of Amur tigers.

Keywords

Panthera tigris altaica; conservation genomics; inbreeding; mutational load; genetic purging

Introduction

Human-induced habitat fragmentation and environmental changes have resulted in a large proportion of biodiversity being reduced to small and isolated populations (Haddad et al., 2015; Said et al., 2016; Khan et al., 2021; Long et al., 2021;). The genetic diversity of a species is of importance for sustaining evolutionary potential, which could help resist the impact of environmental changes and thereby reduce the risk of extinction (Spielman et al., 2004; Markert et al., 2010). The genetic variability in a small population is highly sensitive to genetic drift and inbreeding, which potentially increases genome homozygosity and exacerbates population decline by increased homozygosity of recessive deleterious mutations (Bijlsma et al., 2000; Keller and Waller, 2002; Feng et al., 2019; Dussex et al., 2021). Genetic purging is the pressure from purifying selection against the recessive deleterious mutations due to homozygosis. The inbreeding could facilitate the purging of deleterious mutations and serves an important role in reducing mutational load (genetic burdens) in a population (Xue et al., 2015; Grossen et al., 2020).

The Amur tiger (*Panthera tigris altaica*) is among the most endangered big cats on the planet and has been prioritized for conservation for decades. The wild Amur tiger population has fragmented into three subpopulations, and the subpopulation in China, with about 60 individuals, lives in northeast China and is connected to the two Russian subpopulations (Long et al., 2021). Previous estimations based on microsatellite markers showed that the China subpopulation has been moderately or highly inbred, suggesting a risk of rapid loss of genetic diversity (Ning et al., 2022). China has also established a captive population of the Amur tiger as an *ex situ* conservation resource in the northeast area (Liu et al., 2013). This captive population was initially established in 1986, with eight wild-born founders transported from several zoos in China. Subsequently, this captive population also introduced several individuals from other countries, to improve the population. The wild origins of these individuals at least include both Far Eastern Russia and Northeastern China, but more detailed information for these eight tigers is lacking. Although hybridization among tiger subspecies is common in "farmed" Amur tigers in America (Armstrong et al., 2024), the hybridization in this captive population in northeast China has been strictly managed and recorded for the past 38 years.

Recently, genetic rescue has been proposed to address the issue of inbreeding in wild Amur tigers, with rescue involving genes from captive tigers, as it is known that introducing genetic variation from large, healthy populations can effectively improve genetic diversity in small populations (Weeks et al., 2011; Whiteley et al., 2015; Weeks et al., 2017). Moreover, despite evidence of moderate inbreeding in captive Amur tigers, based on genome-wide screening of runs of homozygosity (ROH) (Zhang et al., 2023), this population seems to be the most suitable source for genetic rescue of wild tigers. Planning genetic rescue largely depends on the comprehensive investigation of genetic backgrounds, including characterization of genetic structure, genetic diversity, and inbreeding in both recipient and source populations, as well as evaluation of the accumulated deleterious mutations across the genome (Xue et al., 2015; Von Seth et al., 2021; Wang et al., 2021; Kardos et al., 2023;). However, the genomic background of wild populations is largely unknown.

To precisely reveal the above-mentioned genetic factors in wild Amur tigers for improving their

protection and conservation, we generated a new representative, high-quality reference genome for the Amur tiger. We conducted a comparative population genomic analysis between wild and captive Amur tigers and explored their genetic structure, genome-wide inbreeding, and genetic diversity, along with the accumulation of mutational load and genetic purging. The insight gained from this study has implications for the future conservation of this species.

Results

Genome assemblies and comparison of haploid genomes

We generated a high-quality chromosome-scale genome assembly (hereafter PtaHapG) for the Amur tiger, providing a new representative reference genome for tigers (Fig.1A; Table 1). The complete X chromosome and a 10.87 Mb Y-linked region were identified and validated by multiple lines of evidence (Figs. 1B, S1A–1D, S2). We also phased scaffolds and obtained two groups of haplotigs for the tiger genome (hereafter PtaHapGH1 and PtaHapGH2) (Figs.1A, S1B, S1C). The Merqury k-mer analysis and BUSCO analysis (Table S1) both revealed that the two groups of haplotigs were highly complete, with a low level of artefactual duplication (Fig. 1C; Table S2). Base-level quality evaluation (Tables S2 and S3) and structural-level accuracy evaluation (Table S4) both supported the high accuracy of genome assemblies.

In general, two haploid genomes (PtaHapGH1 and PtaHapGH2) were found to be very similar with clear one-to-one syntenic blocks between the homologous chromosome pairs (Fig. S3), scarce of haplotype-specific sequences (Fig. 1C). The frequency of sequence differences between the two haploid genomes within 100bp windows showed one peak in the histogram (Fig. S4A), further indicating the high similarity between the two haploid genomes. Nonetheless, we still found some chromosomal SVs between PtaHapGH1 and PtaHapGH2. In total, we found 4463 (2067 deletions, 424 duplications, 34 translocations, and 1938 inversions) SVs between haploid genomes (Table S5). All SVs were supported by genome mapping of both PacBio long reads and DNBSEQ short reads (Fig. S4B). Although 2163 genes were distributed in these SVs, with 1779 genes spanning over breakpoints (Table S6), we did not find that any gene was pseudogenized by the interruption of SVs.

Wild and captive Amur tigers are genetically distinct

The average sequencing depth and coverage for all sampled individuals (Fig. 2A) are 29.92-fold and 98.18%, respectively, and 26.61-fold and 98.69% for wild tiger, respectively (Tables S3 and S7). For the first time, we found that wild and captive Amur tigers formed two distinct clades based on the phylogenetic analysis, which was further supported by Admixture and PCA analysis (Figs. 2B, 2C, S5A), showing a significant genetic difference between wild and captive Amur tigers. By further inspection, we found that captive individuals presented a more scattered state in the PCA result, unlike wild tigers, which exhibited a more aggregate cluster. The genetic diversity calculated from both whole genome analysis (π and heterozygosity) and mitochondrial genome analysis (haplotype diversity, HD) showed a much lower diversity in wild Amur tigers than that in captive individuals (Fig. 2D, 2E, S5B; Table S8). This is in line with the complex but different ancestral origin of the captive tigers from the wild tigers in

China.

Recent demographic history of the wild Amur tiger

We first inferred and described the dynamics of effective population size (N_e) of wild Amur tigers over its evolutionary history. In general, *Ne* for the wild Amur tiger has been declining for a long time, since 300 thousand years ago (kya) (Fig. S6), which is consistent with a previous report on the captive Amur tigers (Zhang et al., 2023). We then explored the population history of Amur tigers during the more recent Anthropocene (the past 100 generations, ~500 years) by using linkage disequilibrium (LD)-based estimates for both wild and captive Amur tigers. The result indicated a relatively small and stable *Ne* of approximately 600 or less from ~100 to ~70 generations ago of the wild population. Within the most recent ~70 generations, the wild population experienced a decrease in *Ne* with less than 50 (Fig. 2F). Considering the possibly different origin, we also inferred the historical population dynamics for these captive Amur tigers. Interestingly, the *Ne* of the captive population has consistently been higher than that of the wild population during the most recent 100 generations. Notably, the *Ne* of the captive population was stable, at approximately or more than 6,000, from 100 to ~40 generations ago, which is 10 times higher than that of the wild tigers. However, the *Ne* began to rapidly decrease in the past 40 generations, before finally reaching a level similar to that of the wild population. This result indicates that these captive tigers may have originated from very different wild progenitor populations 500 years ago (~100 generations ago), and some of the populations may have been extinct in the wild.

Estimates of inbreeding in wild Amur tigers

Here, we quantified inbreeding in both wild and captive Amur tigers by screening genome-wide ROHs. In wild Amur tigers, the average ROH number and length per individual were 1,690.15 ± 36.41 and 689.01 Kb ± 28.04 Kb, respectively, and the longest ROH reached 34.75 Mb. We further found 3457 and 81 ROHs longer than 1Mb and 10 Mb in the wild population (Table S9), accounting for 15.73% and 0.37% of the total ROHs, respectively (Fig. S7A). The above-mentioned estimates in the captive Amur tigers were found to be lower than that in wild Amur tigers. Interestingly, we did not find ROH fragments that were shared by all captive individuals, but 625 ROHs were shared by all 13 wild Amur tigers (Fig. S7B).

We further measured the inbreeding level by ROH-based inbreeding coefficients (F_{ROH}). In general, the F_{ROH} was found to be negatively related to genome-wide heterozygosity in both captive and wild Amur tigers (Fig. 3A), but the overall inbreeding level in the wild Amur tiger is much more severe than in captive individuals (Fig. 3A–3D). The $F_{ROH>100Kb}$, $F_{ROH>1Mb}$, and $F_{ROH>10Mb}$ were 0.50 ± 0.01, 0.32 ± 0.02, and 0.04 ± 0.01 per individual in the wild population, while in captive Amur tigers, we showed 0.24 ± 0.01, 0.14 ± 0.01, and 0.02 ± 0.004 for the same order of F_{ROH} (Fig. 3B; Table S10). It is evident that the wild population is more inbred than captive tigers, up to two times higher, as measured with F_{ROH}. The fraction of ROHs introduced by the recent inbreeding events (the most recent 3 generations) became less frequent in the wild population, but the $F_{ROH>10Mb}$ was still higher than that in captive tigers by two times (Fig. 3B).

To look into the detailed inbreeding history of wild Amur tigers, we dissected the ROH distribution by

length according to Saremi *et al* (Saremi et al., 2019). We found that a large proportion of ROH fragments were restricted to < 1Mb (Fig. 3C). We further observed that the number of ROHs shorter than 10 Mb was much more in the wild Amur tigers than in captive tigers (N_{wild}= 1683.92 ± 37.67, $N_{captive}$= 992.33 ± 16.26, P = 6.8e−12) (Fig. S8; Table S11), signifying that the wild population may have experienced severe inbreeding than captive tigers several generations ago. Likewise, the F_{ROH} with ROH fragments longer than 10 Mb in the wild tigers ($F_{ROH>10Mb}$ = 4.14% ± 0.97%) was also significantly higher than that in captive tigers ($F_{ROH>10Mb}$ = 2.16% ± 0.37%). The average $F_{ROH>10Mb}$ in wild and captive tigers were both smaller than the small isolated Bengal tiger (*P. t. tigris*) population in India ($F_{ROH>10Mb}$ = 28%) (Khan et al., 2021), as well as in the South China tiger (*P. t. amoyensis*) (16%) (Zhang et al., 2023).

Another superiority of our assembly when compared to the unphased genome is that we partitioned the diploid chromosomes into haploid chromosomes. This allowed us to accurately evaluate the switch error rate of the imputed phasing of genotypes, which can then be used to predict future genome homozygosity attributed to inbreeding (Fig. S9). By comparing with the true haploid states phased by the HiFi genome in this study, we estimated a high switch error rate (4.8%) for the imputed phasing by BEAGLE software (Table S12). This result indicates the importance of using haplotype-resolved genome assembling technology for accurate genome phasing, which is potentially valuable to support animal conservation.

Detection of genome-wide mutational load in wild Amur tigers

Mutational load is a kind of intrinsic threat to reduce the fitness of endangered species. Here, we firstly investigated the genome-wide mutational load in protein-coding regions for wild Amur tigers by focusing on deleterious (dnsSNPs), missense mutations, and loss-of-function mutations (LOF), which are expected to potentially affect gene function (Dussex et al., 2021; Von Seth et al., 2021; Yang et al., 2023). We identified 571 nonsynonymous SNPs (Grantham Scores ≥ 150), 9,600 missense mutations, and 121 LOF mutations in the wild population, which was much lower than in captive Amur tigers (N_{dnsSNP} = 1035, $N_{missense}$ = 18,043, and N_{LOF} = 218) (Figs. 4A and S10A; Table S13). We further compared wild and captive populations by using the Rxy method (compare the frequency of derived mutational load in one population relative to the other population) to estimate whether the excess of deleterious derived alleles existed in wild Amur tigers. Rxy results showed a relatively balanced relationship between the wild and captive tigers for intergenic mutations, missense mutations, and dnsSNPs, which presented the neutral state or small fitness effects (Fig. 4B). For LOF mutations, however, we found obviously reduced frequency in wild Amur tigers relative to captive Amur tigers, which suggests that repeated inbreeding in the wild population might facilitate a more efficient purging of large-effect LOF mutations than in captive tigers. Interestingly, the frequency of LOF mutations inside ROH regions was much lower than in non-ROH regions in the wild population but was comparable to captive Amur tigers (Figs. 4C, S10B–S10D). This seems to contradict the results from Rxy analysis, because a more efficient purging should result in a relatively small difference in the frequency of mutational load between ROH and non-ROH regions (Xue et al., 2015; Dussex et al., 2021). We inferred that this may result from the relaxed purifying selection in the captive environment, because tigers with even large-effect deleterious mutations exposed by inbreeding might still survive under human breeding management. In addition, we observed a higher proportion of both derived LOF mutations and dnsSNPs in the homozygous state in wild populations

than in captive Amur tigers (Fig. 4D), indicating that the fitness cost of individual inbreeding in the wild population may be higher than in captive tigers, despite genetic purging.

We further found that the frequency of fixed alleles was much higher in the wild tigers than in captive tigers, and the frequency of derived neutral alleles fixed in the wild tigers (11.03%) was greater than in damaging alleles (8.32%) (Fig. S11; Table S14). This finding indicates that a stronger bottleneck may have occurred in the wild population compared with the captive individuals, which have drifted the rare mutations to a high frequency, here include both the deleterious and neutral mutations. Furthermore, it could be expected that the deleterious alleles in a population should be at a lower frequency than neutral alleles under purifying selection. In this study, we found that, in both wild and captive populations, the average frequency of putatively damaging alleles was lower than that of neutral alleles. We infer that both pressures from purifying selection and the genetic drift are playing roles in the accumulation of mutational load in Amur tigers.

Discussion

Currently, the combination of HiFi reads and HiFi-specific assembler can generate haplotype-resolved *de novo* genomes, representing one of the most promising strategies for genome assembly by far (Cheng et al., 2021; Formenti et al., 2022). The genome we report here provides a new representative high-quality reference genome for the Amur tiger, which has much higher contiguity and less contig number than that of the previously reported Amur tiger genome assemblies, with the contig N50 being of ~692-fold and ~3-fold longer than that of the PanTig1.0 (N50: 0.039 Mb) and PanTig2.0 (N50: 9.52 Mb) (Cho et al., 2013; Mittal et al., 2019) (Table S15). This significant improvement in contiguity will greatly improve the evaluation of inbreeding in tigers. In particular, by comparing this genome to the previously published chromosome-scale genome of a captive Amur tiger (Zhang et al., 2023), we found 37.72 Mb wild Amur tiger-specific sequences harboring the gene *OR56A3*, which was missing in the captive genome. The wild Amur tiger-specific genomic regions were well validated by the population data (Fig. S12). Combined with the estimation of the switch error rate across the genome, we demonstrate the necessity of the HiFi genome in conservation genomics.

Considering the highly inbred Amur tiger population in northeast China (Long et al., 2021; Ning et al., 2022) and the moderately inbred captive Amur tiger population (Liu et al., 2013; Zhang et al., 2023), the captive individuals seem to be a valuable *ex situ* resource for the future conservation of wild Amur tigers. The better inbreeding situation in captive tigers may result from both the complex progenitor populations and a better population management over decades. Here, we found an overwhelming proportion (~99%) of ROHs (>100 Kb) distributed in IBD regions in the wild population, suggested that the majority of ROHs have resulted from inbreeding. Furthermore, ~87% of ROH fragments were restricted to < 1 Mb in the wild population, suggesting inbreeding could be dated back to 26 generations ago (estimated based on a recombination rate of 1.9 cM/Mb from the domestic cat (Li et al., 2016)). The number of ROHs < 5 Mb and ROHs < 10 Mb in wild tiger genomes were both significantly greater than that in captive genomes, signifying that the wild population experienced more extensive inbreeding three to five generations ago. Generally, we showed that the F_{ROH} calculated from ROHs longer than 100 Kb, 1 Mb,

5 Mb, and 10 Mb were all higher in wild tigers than in captive tigers by 2.12, 2.24, 2.15, and 1.92 times, and the number of ROHs shared among wild Amur tigers was much higher than that in captive Amur tigers, both suggesting more intensive inbreeding in wild Amur tigers over the most recent ~260 generations (>100Kb ROH). Fortunately, the overall inbreeding in both wild and captive Amur tigers has been becoming less frequent over the most recent 130 years (5 years per generation) when compared with other tiger subspecies (Fig. S13). In particular, the average F_{ROH} > 10 Mb was only ~4% in the wild Amur tiger population, which is much lower than that of the South China tiger (*P. t. amoyensis*) (F_{ROH} = 16%) (Zhang et al., 2023) and the small isolated Bengal tiger (*P. t. tigris*) population in India (F_{ROH} = 28%) (Khan et al., 2021). This suggests that the negative effects of recent inbreeding may not be very serious yet, potentially because of recent protection and management efforts. However, this high inbreeding level in the small tiger population will undoubtedly lead to a loss of population-level adaptive potential and even to extinction without timely conservation.

Although overall inbreeding in wild Amur tigers was much higher than in captive Amur tigers, we found that the mutational load in wild tigers is much lower than in captive tigers (Fig. 4A). Expectedly, this might be result from genetic purging promoted by inbreeding and maintained by the purifying selection (Dussex et al., 2021; Khan et al., 2021; Kleinman-Ruiz et al., 2022; Zhang et al., 2023). In this study, we found a relatively reduced number of LOF mutations (Fig. 4B) but not dnsSNPs and missense mutations in wild Amur tigers. This may be explained by more efficient genetic purging of relatively large-effect deleterious mutations in wild Amur tigers, relative to captive individuals. However, we still found a much higher ratio of homozygous LOF mutations in the wild population than the captive population, indicating that genetic purging is not sufficient to keep a lower fitness cost in wild tigers. The more fixed putatively damaging alleles in the wild Amur tigers also supported a less efficient genetic purging (Fig. S11).

Although the population number of wild Amur tigers has been successfully restored in the past decade (National Forestry and Grassland Administration, China, 2022), their security is still a cause for concern. The next phase of conservation efforts should focus on reducing inbreeding, which is a major threat to the long-term survival of the species. One immediate and necessary approach is to build ecological corridors to connect population patches within China and Russia. This would help to eliminate landscape resistance of migration and improve gene flow between different populations (Long et al., 2021) and will serve as key infrastructure supporting their long-term survival (Ćurčić and Đurđić, 2013). The second and parallel approach is genetic rescue using a healthier captive population (Ralls et al., 2020). We found that captive tigers are genetically distant from the wild tigers and higher in genetic diversity (Figs. 2B–2E, S5). This different genetic background between the captive tigers and wild tigers may result from the captive population having been established via collections from multiple ancestor populations, including from sites that no longer have wild populations, potentially making these animals a very valuable genetic resource. However, captive Amur tigers carry a greater mutational load (Fig. 4A), a considerable proportion of which is absent in the wild population (Fig. S14; Table S13). By simply simulating reintroduction of captive tigers to the wild population for genetic rescue, we predicted that 411 derived dnsSNPs and 119 LOF mutations are likely to be introduced into the wild population (Fig. S15). This suggests that introducing captive individuals into the wild population may be risky, since it can simultaneously introduce a novel mutational load that may have further negative impacts. Fortunately,

the introduced mutations vary depending on gene donors, leaving more possibilities for selecting the optimal candidate tiger. In this study, we established a partial list of the deleterious mutations for Amur tigers. With the aim of real genetic rescue, the list of mutational load should be completed by sampling more wild tigers and potential captive gene donors.

Materials and methods

Samples and genome sequencing

We collected a blood sample from a rescued wild male Amur tiger from Heilongjiang Province, China, for high-molecular-weight DNA isolation and genome assembly. Thirteen more wild Amur tiger samples (12 feces and 1 blood) and 17 captive Amur tigers (feces samples) from Heilongjiang Siberian Tiger Park were collected for regular DNA isolation for whole genome re-sequencing. Blood samples were collected by anticoagulation tube from rescued individuals in the wild after anesthesia treatment and were immediately transferred to liquid nitrogen. Samples were stored at –80°C. Feces samples were collected from the field work and stored at –80°C until DNA isolation. In addition, we downloaded whole genome sequencing data of 13 captive Amur tigers for genomic analysis (Zhang et al., 2023). DNA isolation and library preparation for blood and feces samples were conducted according to the manufacturer's instructions of commercial kits (Supplementary materials). Paired-end sequencing of 100bp reads was performed on a DNBSEQ T1 sequencer (MGI, Shenzhen, China).

Genome assembly, assessment and annotation

The genome size was estimated by kmerfreq (v2.4) (https://github.com/fanagislab/kmerfreq) with ~50-fold short reads for the Amur tiger (Fig. S1A). The chromosome-level genome was assembled by hifiasm (Cheng et al., 2021) (v0.16.1) with PacBio and Hi-C sequencing data. Benchmarking Universal Single-Copy Orthologs (BUSCO) (Manni et al., 2021) (v5.2.2) analysis was performed to evaluate the completeness of the tiger genome with mammalia_odb10 database. The genome assembly accuracy was evaluated by both Merqury (Rhie et al., 2020) (release 20200430) k-mer analysis and PacBio long reads alignments. For the genome annotation, we firstly used the *de novo* and homolog-based methods to annotate repeat elements. Protein-coding genes were further annotated with *de novo*, homology-based and transcript-based evidence after masking repeat elements across the genome. The final gene set representing RNA-seq, homology, and *de novo*-predicted genes was generated by via the MAKER pipeline (Campbell et al., 2014) (v3.01.03). For functional annotation, we performed a BLAST search against the SwissProt, TrEMBL, and Kyoto Encyclopedia of Genes and Genomes (KEGG) database, with an E-value cut-off of 1e-5 (see Supplementary information).

Genome-wide variants calling and quality control

For wild feces samples, we first performed species identification using BLAST alignment of sequencing reads to the nucleotide database of NCBI and confirmed that all feces samples we collected are from the Amur tiger. Then, the BWA *mem* algorithm (Li, 2013) was used to map the whole genome resequencing data of all Amur tiger individuals to the PtaHapG genome with default parameters. Sentieon (Freed et al., 2017) (v202010.01) was used for sorting, reordering, and deduplication of alignment files for the

following variants calling. Variants were first identified by Sentieon (Freed et al., 2017) (v202010.01) DNAseq HaplotypeCaller pipeline for each individual, and the following joint calling was carried out by Sentieon DNAseq GVCFtyper with gVCF files to create a common VCF file. To facilitate downstream analysis, we only retained the bi-allelic single nucleotide polymorphism (SNP) in the variant set. For SNP quality control, we firstly performed hard filtration with parameters of "QD <2.0 || FS > 60.0 || MQ < 40.0 || MQRankSum < -12.5 || ReadPosRankSum < -8.0" (DePristo et al., 2011). Then, we removed the SNPs with the top and bottom 0.5% sequencing depth and SNPs with a missing rate greater than 20%. In addition, we removed all SNPs in both X and Y chromosomes for downstream analysis.

Population structure analysis and genomic diversity

Before population genomic analysis, we first identify the kinship coefficient by the KING (Manichaikul et al., 2010) (v2.2.4) software to remove recaptured feces samples or closely related individuals. We found three feces samples that were duplicated and subsequently removed from the analysis. We finally retained 13 unrelated wild tiger individuals for the downstream analysis. For PCA analysis, we used the PLINK (Purcell et al., 2007) (v1.90b6.10) software to convert VCF file to PLINK format file, and then PCA was performed using Genome-wide Complex Trait Analysis (GCTA) (Yang et al., 2011) (v1.92.2) with default parameters. For the construction of a phylogenetic tree, we first used vcf2phylip (Ortiz, 2019) (v2.7) to convert the VCF file into PHYLIP format. Then, we selected the best substitution model to construct the maximum likelihood (ML) phylogenetic tree using IQ-TREE (Nguyen et al., 2015) (v1.6.12) with default parameters. ADMIXTURE (Alexander et al., 2009) (v1.3.0) was used to determine the ancestry proportion of tiger individuals from a specified number of clusters (K) from 1 to 10. The best K value we estimated was 2 by CV error analysis. We used vcftools (Danecek et al., 2011) (v0.1.16) with parameters of "vcftools --gzvcf vcf.gz --window-pi 1000000 -out result" for genome-wide π analysis and "vcftools --gzvcf vcf.gz --het --out result" for genome-wide heterozygosity calculation.

ROH and IBD detection

Before ROH detection, we firstly converted the multi-individual VCF file into PLINK bfile format by the PLINK (Purcell et al., 2007) (v1.90b6.10) software. Then, ROH regions in captive and wild Amur tigers were detected using the PLINK (Purcell et al., 2007) (v1.90b6.10) software with parameters of "--homozyg --homozyg-window-snp 20 --homozyg-kb 10 --homozyg-density 50" (Dobrynin et al., 2015). ROH fragments shorter than 100 kb were dropped in this study. The F_{ROH} was calculated by formula $F_{ROH} = L_{ROH}/L_{AUTOSOME}$. L_{ROH} was the total length of ROHs across the autosomes in each individual, $L_{AUTOSOME}$ was the total length of the autosomes. We used the formula $g = 100/2rL_{ROH}$ to infer the time (by generation) of ROH generated, where the g = generation interval, r = recombination rate (here we used 1.9 cM/Mb from the domestic cat (Li et al., 2016)), and the L_{ROH} = length of the ROH in Mb. We detected the IBD blocks of all individuals by using Refined IBD (Browning and Browning, 2013) (v17Jan20.102) with default settings.

Population demography inference

SMC++ (Terhorst et al., 2017) (v1.5.1) was performed to infer the change of effective population size along evolutionary history with all wild Amur tiger individuals. We visualized the SMC++ results by

scaling the time to the real years by using the generation time of 5 years and mutation rate of $\mu_{amur\ tiger} = 3 \times 10^{-9}$ for the Amur tiger (Liu et al., 2018; Paijmans et al., 2021). The recent change of effective population size (Ne) of wild and captive Amur tigers was analyzed using GONE (Santiago et al., 2020) software (available at https://github.com/esrud/GONE), following the parameters set by Kardos et al (Kardos et al., 2023) and adjusted the *hc* parameter to 0.02 to mitigate potential bias in the recent population substructure. We ensured the robustness of our results by replicating the analysis 500 times, each iteration varying the set of 10,000 SNPs per chromosome.

Mutational load and site-frequency spectrum (SFS) analysis

For screening mutational load in protein-coding genes, we annotated variants with ANNOVAR (Wang et al., 2010) (v20191024) and SnpEff (Cingolani et al., 2012) (v.5.0e) software. Variants annotated as stop gained, splice acceptor, and splice donor by SnpEff (Cingolani et al., 2012) were predicted as LOF. Meanwhile, SNPs annotated as missense_variant, synonymous_variant, and intergenic by SnpEff were identified as missense, synonymous, and intergenic variants, respectively. Non-synonymous SNPs with Grantham Scores ≥150 were regarded as dnsSNP (Grantham, 1974). The frequency of mutational load in ROH and non-ROH regions for each individual genome was calculated by dividing the total number of deleterious mutations within ROH or non-ROH regions by the number of synonymous mutations in the corresponding regions. For the SFS analysis, the intergenic variants were defined as neutral mutation, while LOF and missense variants were predicted as putatively damaging mutations, according to the previous study (Khan et al., 2021). We randomly selected 10 individuals from each population for SFS analysis and performed three replicates. Then, we estimated the derived neutral and derived putatively damaging allele frequencies at each locus in each population (Khan et al., 2021) (see Supplementary information).

Ethics

Sample collection, experiments, and research design were approved by the Institutional Review Board of BGI (BGI-IRB E22017)

Data Availability

The data that support the findings in this study have been deposited into CNGB Sequence Archive (CNSA) (Guo et al., 2020) of China National GeneBank DataBase (CNGBdb) (Chen et al., 2020) with accession number CNP0003803. The raw sequencing data has also been deposited in the Genome Sequence Archive under the accession number CRA020608 (https://ngdc.cncb.ac.cn/gsa/browse/CRA020608).

CRediT authorship contribution statement

Tianming Lan: Conceptualization, Writing - Original draft, Writing - Review & Editing, Project administration. **Haimeng Li**: Methodology, Formal analysis, Data curation, Writing - Original draft. **Boyang Liu**: Formal analysis, Investigation, Writing - Original draft, Visualization. **Minhui Shi**: Formal

analysis, Visualization. **Yinping Tian**: Formal analysis. **Sunil Kumar Sahu**: Writing - Review & Editing. **Liangyu Cui**: Investigation, Methodology. **Nicolas Dussex**: Writing - Review & Editing. **Dan Liu**: Resources. **Yue Ma**: Investigation. **Weiyao Kong**: Resources. **Shanlin Liu**: Writing - Review & Editing. **Jiale Fan**: Investigation. **Yue Zhao:** Resources. **Yuan Fu:** Formal analysis. **Qiye Li**: Writing - Review & Editing. **Chen Lin**: Investigation. **Love Dalén**: Writing - Review & Editing. **Huan Liu**: Conceptualization, Writing - Review & Editing, Funding acquisition. **Le Zhang**: Formal analysis, Investigation, Writing - Review & Editing. **Guangshun Jiang**: Conceptualization, Writing - Review & Editing. **Yanchun Xu**: Conceptualization, Writing - Review & Editing, Supervision, Funding acquisition.

Conflict of interest

The authors declare no competing interests.

Acknowledgments

This study was supported by the Fundamental Research Funds for the Central Universities of China (2572022DQ03), National Natural Science Foundation of China (32170517), the Guangdong Provincial Key Laboratory of Genome Read and Write (grant No. 2017B030301011) and the Start-up Scientific Foundation of Northeast Forestry University (60201524043). This work was also supported by China National GeneBank (CNGB).

References

Alexander, D.H., Novembre, J., Lange, K., 2009. Fast model-based estimation of ancestry in unrelated individuals. Genome Res. 19, 1655-1664.

Armstrong, E.E., Mooney, J.A., Solari, K.A., Kim, B.Y., Barsh, G.S., Grant, V.B., Greenbaum, G., Kaelin, C.B., Panchenko, K., Pickrell, J.K., 2024. Unraveling the genomic diversity and admixture history of captive tigers in the United States. Proc. Natl. Acad. Sci. U. S. A. 121, e2402924121.

Bijlsma, Bundgaard, Boerema, 2000. Does inbreeding affect the extinction risk of small populations?: predictions from Drosophila. J. Evol. Biol. 13, 502-514.

Browning, B.L., Browning, S.R., 2013. Improving the accuracy and efficiency of identity-by-descent detection in population data. Genetics 194, 459-471.

Campbell, M.S., Holt, C., Moore, B., Yandell, M., 2014. Genome annotation and curation using MAKER and MAKER-P. Curr. Protoc. bioinformatics 48, 4.11. 11-14.11. 39.

Chen, F.Z., You, L.J., Yang, F., Wang, L.N., Guo, X.Q., Gao, F., Hua, C., Tan, C., Fang, L., Shan, R.Q., 2020. CNGBdb: China National GeneBank DataBase. Yi Chuan 42, 799-809.

Cheng, H., Concepcion, G.T., Feng, X., Zhang, H., Li, H., 2021. Haplotype-resolved de novo assembly using phased assembly graphs with hifiasm. Nat. Methods 18, 170-175.

Cho, Y.S., Hu, L., Hou, H., Lee, H., Xu, J., Kwon, S., Oh, S., Kim, H.-M., Jho, S., Kim, S., 2013. The tiger genome and comparative analysis with lion and snow leopard genomes. Nat. Commun. 4, 1-7.

Cingolani, P., Platts, A., Wang, L.L., Coon, M., Nguyen, T., Wang, L., Land, S.J., Lu, X., Ruden, D.M., 2012. A program for annotating and predicting the effects of single nucleotide polymorphisms, SnpEff: SNPs in the genome of Drosophila melanogaster strain w1118; iso-2; iso-3. fly 6, 80-92.

Ćurčić, N., Đurđić, S., 2013. The actual relevance of ecological corridors in nature conservation. Zbornik radova Geografskog instituta" Jovan Cvijić", SANU 63, 21-34.

Danecek, P., Auton, A., Abecasis, G., Albers, C.A., Banks, E., DePristo, M.A., Handsaker, R.E., Lunter, G., Marth, G.T., Sherry, S.T., 2011. The variant call format and VCFtools. Bioinformatics 27, 2156-2158.

DePristo, M.A., Banks, E., Poplin, R., Garimella, K.V., Maguire, J.R., Hartl, C., Philippakis, A.A., Del Angel, G., Rivas, M.A., Hanna, M., 2011. A framework for variation discovery and genotyping using next-generation DNA sequencing data. Nat. Genet. 43, 491-498.

Dobrynin, P., Liu, S., Tamazian, G., Xiong, Z., Yurchenko, A.A., Krasheninnikova, K., Kliver, S., Schmidt-Küntzel, A., Koepfli, K.-P., Johnson, W., 2015. Genomic legacy of the African cheetah, Acinonyx jubatus. Genome Biol. 16, 1-20.

Dussex, N., Van Der Valk, T., Morales, H.E., Wheat, C.W., Díez-del-Molino, D., Von Seth, J., Foster, Y., Kutschera, V.E., Guschanski, K., Rhie, A., 2021. Population genomics of the critically endangered kākāpō. Cell Genomics 1.

Feng, S., Fang, Q., Barnett, R., Li, C., Han, S., Kuhlwilm, M., Zhou, L., Pan, H., Deng, Y., Chen, G., 2019. The genomic footprints of the fall and recovery of the crested ibis. Curr. Biol. 29, 340-349. e347.

Formenti, G., Theissinger, K., Fernandes, C., Bista, I., Bombarely, A., Bleidorn, C., Ciofi, C., Crottini, A., Godoy, J.A., Höglund, J., 2022. The era of reference genomes in conservation genomics. Trends Ecol. Evol. 37, 197-202.

Freed, D., Aldana, R., Weber, J.A., Edwards, J.S., 2017. The Sentieon Genomics Tools–A fast and accurate solution to variant calling from next-generation sequence data. BioRxiv, 115717.

Grantham, R., 1974. Amino acid difference formula to help explain protein evolution. science 185(4154), 862-864.

Grossen, C., Guillaume, F., Keller, L.F., Croll, D., 2020. Purging of highly deleterious mutations through severe bottlenecks in Alpine ibex. Nat. Commun. 11, 1001.

Guo, X., Chen, F., Gao, F., Li, L., Liu, K., You, L., Hua, C., Yang, F., Liu, W., Peng, C., 2020. CNSA: a data repository for archiving omics data. Database 2020, baaa055.

Haddad, N.M., Brudvig, L.A., Clobert, J., Davies, K.F., Gonzalez, A., Holt, R.D., Lovejoy, T.E., Sexton, J.O., Austin, M.P., Collins, C.D., 2015. Habitat fragmentation and its lasting impact on Earth's ecosystems. Sci. Adv. 1, e1500052.

Kardos, M., Zhang, Y., Parsons, K.M., Kang, H., Xu, X., Liu, X., Matkin, C.O., Zhang, P., Ward, E.J., Hanson, M.B., 2023. Inbreeding depression explains killer whale population dynamics. Nat. Ecol. Evol. 7, 675-686.

Keller, L.F., Waller, D.M., 2002. Inbreeding effects in wild populations. Trends Ecol. Evol. 17, 230-241.

Khan, A., Patel, K., Shukla, H., Viswanathan, A., van der Valk, T., Borthakur, U., Nigam, P., Zachariah, A., Jhala, Y.V., Kardos, M., 2021. Genomic evidence for inbreeding depression and purging of deleterious genetic variation in Indian tigers. Proc. Natl. Acad. Sci. U. S. A. 118, e2023018118.

Kleinman-Ruiz, D., Lucena-Perez, M., Villanueva, B., Fernández, J., Saveljev, A.P., Ratkiewicz, M.,

Schmidt, K., Galtier, N., García-Dorado, A., Godoy, J.A., 2022. Purging of deleterious burden in the endangered Iberian lynx. Proc. Natl. Acad. Sci. U. S. A. 119, e2110614119.

Li, G., Hillier, L.W., Grahn, R.A., Zimin, A.V., David, V.A., Menotti-Raymond, M., Middleton, R., Hannah, S., Hendrickson, S., Makunin, A., 2016. A high-resolution SNP array-based linkage map anchors a new domestic cat draft genome assembly and provides detailed patterns of recombination. G3, 6, 1607-1616.

Li, H., 2013. Aligning sequence reads, clone sequences and assembly contigs with BWA-MEM. arXiv preprint arXiv:1303.3997.

Liu, D., Ma, Y., Li, H., Xu, Y., Zhang, Y., Dahmer, T., Bai, S., Wang, J., 2013. Simultaneous polyandry and heteropaternity in tiger (Panthera tigris altaica): Implications for conservation of genetic diversity in captive populations of felids. Chinese Science Bulletin 58, 2230-2236.

Liu, Y.-C., Sun, X., Driscoll, C., Miquelle, D.G., Xu, X., Martelli, P., Uphyrkina, O., Smith, J.L., O'Brien, S.J., Luo, S.-J., 2018. Genome-wide evolutionary analysis of natural history and adaptation in the world's tigers. Curr. Biol. 28, 3840-3849.

Long, Z., Gu, J., Jiang, G., Holyoak, M., Wang, G., Bao, H., Liu, P., Zhang, M., Ma, J., 2021. Spatial conservation prioritization for the Amur tiger in Northeast China. Ecosphere 12, e03758.

Manichaikul, A., Mychaleckyj, J.C., Rich, S.S., Daly, K., Sale, M., Chen, W.-M., 2010. Robust relationship inference in genome-wide association studies. Bioinformatics 26, 2867-2873.

Manni, M., Berkeley, M.R., Seppey, M., Simão, F.A., Zdobnov, E.M., 2021. BUSCO update: novel and streamlined workflows along with broader and deeper phylogenetic coverage for scoring of eukaryotic, prokaryotic, and viral genomes. Mol. Biol. Evol. 38, 4647-4654.

Markert, J.A., Champlin, D.M., Gutjahr-Gobell, R., Grear, J.S., Kuhn, A., McGreevy, T.J., Roth, A., Bagley, M.J., Nacci, D.E., 2010. Population genetic diversity and fitness in multiple environments. BMC Evol. Biol. 10, 1-13.

Mittal, P., Jaiswal, S.K., Vijay, N., Saxena, R., Sharma, V.K., 2019. Comparative analysis of corrected tiger genome provides clues to its neuronal evolution. Sci. Rep. 9, 18459.

Nguyen, L.-T., Schmidt, H.A., Von Haeseler, A., Minh, B.Q., 2015. IQ-TREE: a fast and effective stochastic algorithm for estimating maximum-likelihood phylogenies. Mol. Biol. Evol. 32, 268-274.

Ning, Y., Roberts, N., Qi, J., Peng, Z., Long, Z., Zhou, S., Gu, J., Hou, Z., Yang, E., Ren, Y., 2022. Inbreeding status and implications for Amur tigers. Animal Conservation 25, 521-531.

Ortiz, E.M., 2019. vcf2phylip v2. 0: convert a VCF matrix into several matrix formats for phylogenetic analysis. Zenodo Geneva.

Paijmans, J.L., Barlow, A., Becker, M.S., Cahill, J.A., Fickel, J., Förster, D.W., Gries, K., Hartmann, S., Havmøller, R.W., Henneberger, K., 2021. African and Asian leopards are highly differentiated at the genomic level. Curr. Biol. 31, 1872-1882.

Purcell, S., Neale, B., Todd-Brown, K., Thomas, L., Ferreira, M.A., Bender, D., Maller, J., Sklar, P., De Bakker, P.I., Daly, M.J., 2007. PLINK: a tool set for whole-genome association and population-based linkage analyses. Am. J. Hum. Genet. 81, 559-575.

Ralls, K., Sunnucks, P., Lacy, R.C., Frankham, R., 2020. Genetic rescue: A critique of the evidence supports maximizing genetic diversity rather than minimizing the introduction of putatively harmful genetic variation. Biol. Conservation 251, 108784.

Rhie, A., Walenz, B.P., Koren, S., Phillippy, A.M., 2020. Merqury: reference-free quality, completeness, and phasing assessment for genome assemblies. Genome Biol. 21, 1-27.

Said, M.Y., Ogutu, J.O., Kifugo, S.C., Makui, O., Reid, R.S., de Leeuw, J., 2016. Effects of extreme land fragmentation on wildlife and livestock population abundance and distribution. J. Nat. Conservation 34, 151-164.

Santiago, E., Novo, I., Pardiñas, A.F., Saura, M., Wang, J., Caballero, A., 2020. Recent demographic history inferred by high-resolution analysis of linkage disequilibrium. Mol. Biol. Evol. 37, 3642-3653.

Saremi, N.F., Supple, M.A., Byrne, A., Cahill, J.A., Coutinho, L.L., Dalén, L., Figueiró, H.V., Johnson, W.E., Milne, H.J., O'Brien, S.J., 2019. Puma genomes from North and South America provide insights into the genomic consequences of inbreeding. Nat. Commun. 10, 4769.

Spielman, D., Brook, B.W., Frankham, R., 2004. Most species are not driven to extinction before genetic factors impact them. Proceedings of the National Academy of Sciences 101, 15261-15264.

Terhorst, J., Kamm, J.A., Song, Y.S., 2017. Robust and scalable inference of population history from hundreds of unphased whole genomes. Nat. Genet. 49, 303-309.

Von Seth, J., Dussex, N., Díez-del-Molino, D., Van Der Valk, T., Kutschera, V.E., Kierczak, M., Steiner, C.C., Liu, S., Gilbert, M.T.P., Sinding, M.-H.S., 2021. Genomic insights into the conservation status of the world's last remaining Sumatran rhinoceros populations. Nat. Commun. 12, 2393.

Wang, K., Li, M., Hakonarson, H., 2010. ANNOVAR: functional annotation of genetic variants from high-throughput sequencing data. Nucleic Acids Res. 38, e164-e164.

Wang, P., Burley, J.T., Liu, Y., Chang, J., Chen, D., Lu, Q., Li, S.-H., Zhou, X., Edwards, S., Zhang, Z., 2021. Genomic consequences of long-term population decline in brown eared pheasant. Mol. Biol. Evol. 38, 263-273.

Weeks, A.R., Heinze, D., Perrin, L., Stoklosa, J., Hoffmann, A.A., van Rooyen, A., Kelly, T., Mansergh, I., 2017. Genetic rescue increases fitness and aids rapid recovery of an endangered marsupial population. Nat. Commun. 8, 1071.

Weeks, A.R., Sgro, C.M., Young, A.G., Frankham, R., Mitchell, N.J., Miller, K.A., Byrne, M., Coates, D.J., Eldridge, M.D., Sunnucks, P., 2011. Assessing the benefits and risks of translocations in changing environments: a genetic perspective. Evol. Appl. 4, 709-725.

Whiteley, A.R., Fitzpatrick, S.W., Funk, W.C., Tallmon, D.A., 2015. Genetic rescue to the rescue. Trends Ecol. Evol. 30, 42-49.

Xue, Y., Prado-Martinez, J., Sudmant, P.H., Narasimhan, V., Ayub, Q., Szpak, M., Frandsen, P., Chen, Y., Yngvadottir, B., Cooper, D.N., 2015. Mountain gorilla genomes reveal the impact of long-term population decline and inbreeding. Science 348, 242-245.

Yang, J., Lee, S.H., Goddard, M.E., Visscher, P.M., 2011. GCTA: a tool for genome-wide complex trait analysis. Am. J. Hum. Genet. 88, 76-82.

Yang, S., Lan, T., Zhang, Y., Wang, Q., Li, H., Dussex, N., Sahu, S.K., Shi, M., Hu, M., Zhu, Y., 2023. Genomic investigation of the Chinese alligator reveals wild-extinct genetic diversity and genomic consequences of their continuous decline. Mol. Ecol. Res. 23, 294-311.

Zhang, L., Lan, T., Lin, C., Fu, W., Yuan, Y., Lin, K., Li, H., Sahu, S.K., Liu, Z., Chen, D., 2023. Chromosome-scale genomes reveal genomic consequences of inbreeding in the South China tiger: A comparative study with the Amur tiger. Mol. Ecol. Res. 23, 330-347.

559 **Table 1.** Statistics of the sequencing data, assembly, and annotation of the Amur tiger genome.
560

Item	Category	PtaHapG
Sequencing data	PacBio (Gb)	75.79
	WGS (Gb)	216.11
	Hi-C (Gb)	220.45
	RNA-seq (Gb)	62.67
Genome assembly	Estimated genome size (Gb)	2.47
	Assembled genome size (Gb)	2.44
	Contig N50 (Mb)	26.97
	Scaffold N50 (Mb)	147.84
	Longest scaffold (Mb)	239.60
	GC content (%)	41.82
Annotation	Repeat sequences (%)	35.46
	Number of protein-coding genes	19,786
	Number of functionally annotated genes	19,771

561
562

Figure legends.

Fig. 1. Genomic landscapes and haploid genome characteristics of the Amur tiger. **A**: The genomic landscape of the Amur tiger genome. **B**: Averaged depth ratios of re-sequenced male and female individuals for all scaffolds in the PtaHapG. Each blue plot represents an autosome. **C**: K-mer spectra plot for the two haploid genomes of Amur tiger produced by Merqury. Almost all haploid-specific k-mers presented as single-copy (~24X) in the genome, but the shared k-mers by the two haploid genomes presented two-copy (~49X) in the genomes.

Fig. 2. Genetic structure, genetic diversity, and population demography of Amur tigers. **A**: The current distribution area and sampling sites of wild Amur tigers in this study. This image is based on the standard map with the ID GS(2021)5452 that was taken from the website of the National Platform for Common Geospatial Information Services. **B**: Phylogenetic tree constructed by whole genome sequencing data of captive and wild Amur tigers. **C**: PCA clustering of wild and captive Amur tigers. **D**: Comparison of genome-wide heterozygosity between captive and wild Amur tigers. **E**: Network analysis of mitochondrial haplotypes of Amur tigers. **F**: The dynamic of effective population size in the evolutionary history of wild and captive Amur tigers.

Fig. 3. Genome-wide inbreeding estimation of Amur tigers. **A**: A negative relationship between the heterozygosity and F_{ROH} in Amur tiger. Wild Amur tigers are represented in light green, and captive tigers are in green. **B**: The comparison of averaged F_{ROH} in wild and captive Amur tigers. **C**: The length distribution of ROH fragments in Amur tigers. The wild Amur tiger had a high number of ROH fragments shorter than 10 Mb; the corresponding relationship between ROH length and occurrence time scaled by generations is shown. **D**: The distribution of ROH fragments larger than 1Mb across the genome in wild and captive Amur tigers.

Fig. 4. Characteristics of mutational load in captive and wild Amur tigers. **A**: Comparisons of the number of derived mutation load (LOF and dnsSNP) in captive and wild Amur tiger populations. **B**: The Rxy ratio between derived alleles in wild (*x*) and captive (*y*) Amur tigers for intergenic, dnsSNP, missense, and LOF mutations. The Rxy <1 indicates that population *x* has fewer derived alleles than population *y*. **C**: The comparison of frequency of derived LOF variants (LOF number / total number of synonymous in ROH or non-ROH genomic regions) between inside and outside ROH regions. **D**: The proportion of homozygous LOF mutations and dnsSNPs in wild and captive Amur tigers. The proportion of homozygous mutations was calculated with the formula: 2 × homozygous sites / (2 × homozygous sites + heterozygous site).

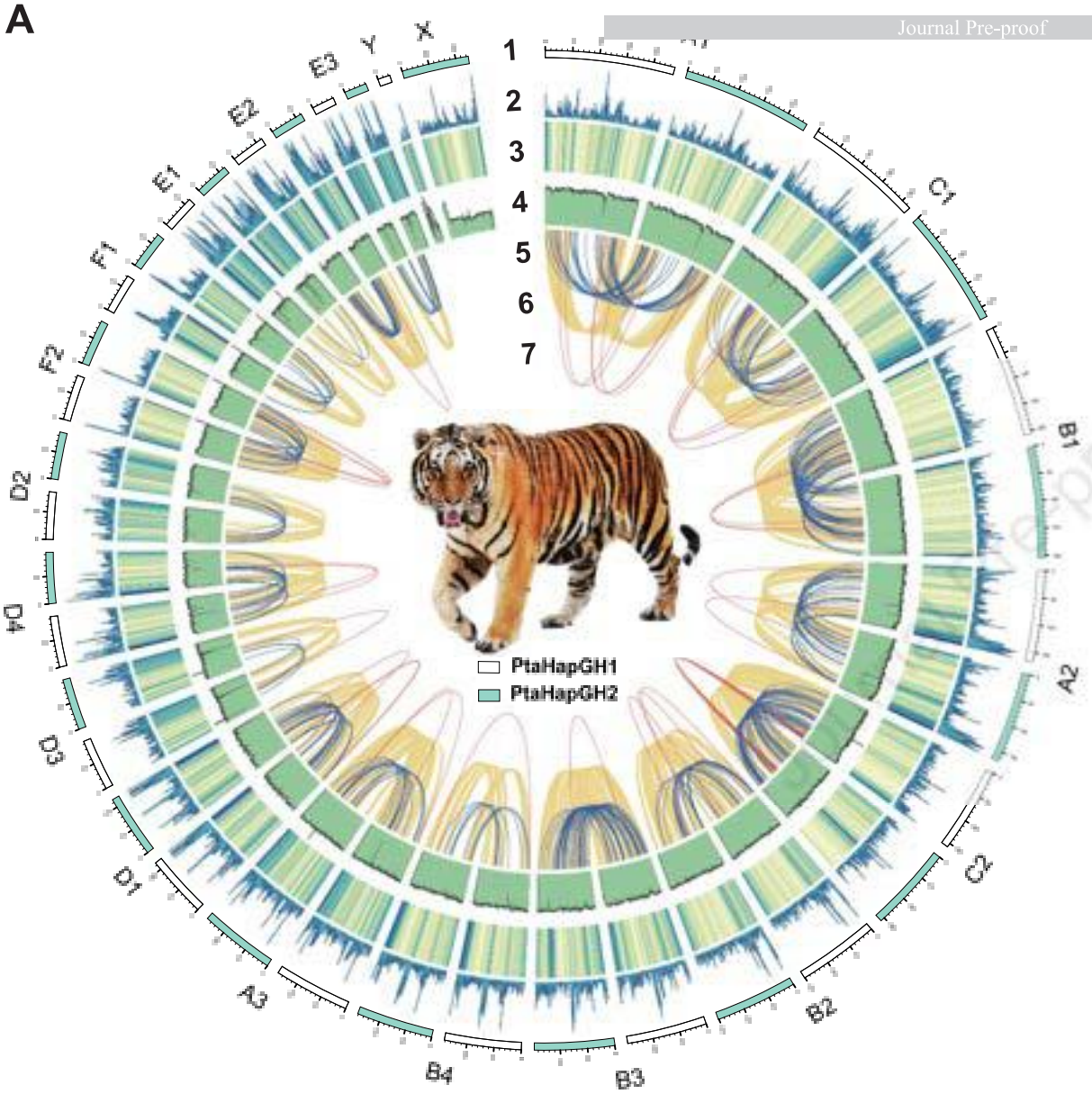

1: schematic diagram of chromosomes (white: PtaHapGH1; green: PtaHapGH2);
2: gene density: 0~30 (per 500 Kb)
3: sequencing depth: 1~100x (per 500 Kb)
4: GC contents:
5: SV: duplication; 6: SV: inversion; 7: SV: translocation.mosomes